Journal of Alloys and Compounds 501 (2010) 193–197

Contents lists available at ScienceDirect

Journal of Alloys and Compounds

journal homepage: www.elsevier.com/locate/jallcom

Persistent UV phosphors for application in photo catalysis

F. Gutiérrez-Martín[a,*], F. Fernández-Martinez[a], P. Díaz[a], C. Colón[b], A. Alonso-Medina[b]

[a] Dep. Química Industrial y Polímeros, EUIT Industrial, Universidad Politécnica de Madrid, Rda. Valencia 3, E-28012 Madrid, Spain
[b] Dep. Física Aplicada, EUIT Industrial, Universidad Politécnica de Madrid, Rda. Valencia 3, E-28012 Madrid, Spain

ARTICLE INFO

Article history:
Received 23 October 2009
Received in revised form 16 April 2010
Accepted 25 April 2010
Available online 5 May 2010

Keywords:
Phosphors
Optical properties
Luminescence
X-ray diffraction

ABSTRACT

Ce^{3+}-doped strontium alumino-silicates $(Sr_{1-v}M_v)_{1+y}Al_{2-x}B_xSi_yO_{4+3y}$ (M:Ca,Mg,Ba) were prepared using solid-state reactions at 1200 °C for 2 h in a weakly reductive atmosphere of 5% H_2-95% N_2. The X-ray diffraction measurements revealed that the products have a good crystallization, and the resultant phosphors show broad emissions centered at 400 nm, with a long-persistence of several minutes ($k = 0.02–0.10\ s^{-1}$). These luminescent properties are considered good enough for novel applications in photo catalysis, which will be the objective of further developments.

1. Introduction

Phosphors that exhibit a long decay time can be discussed in terms of practical applications and mechanisms of generation. They are a kind of energy-storing materials which can absorb light and then release the energy after the excitation sources are removed (usually 'UV irradiation'). However, progress in the development of long afterglow materials has been relatively recent, and—because the mechanisms are complex—there are no general techniques that allow the synthesis of persistent phosphors with designated coloration and/or lifetimes; consideration of the main factors affecting phosphorescence, i.e., the luminescent center and traps, together with practical experience can be used in formulating synthetic strategies [1–3].

There is a strong desire for excellent short wavelength long-lasting phosphors, with maximum emitting values located at about 400 nm or lower, as they can serve as excitation source of other light sensible materials; in particular, these phosphors would find applications in photo catalysis (e.g., it is a possible way to solve the problem of TiO_2 semiconductors, which only show activity under irradiation corresponding to the 387 nm band gap, when the appropriate phosphor is used as photonic source together with the catalyst).

Long-lasting phosphorescence has been observed from several ions in various oxysalt materials (mainly the alkaline-earth aluminates and silicates), where trapping processes involve switching from different valences of lanthanides as doping agents; though only visible emission colors are typically obtained from these structures (e.g., violet, blue, green, red, pink, orange or yellow) [4].

Thus, rare-earth doped materials are good candidates for photonic sources, while Ce^{3+} in ionic crystals is regarded as an optically active ion which emits in the UV/blue spectra regions, based on 4f–5d transitions; e.g. $MgAl_2O_4$ exhibits a persistent afterglow at 520 nm from V_K^{3+} centers, but this is greatly enhanced by Ce^{3+} doping (peaking at 405 nm) [5]. $CaAl_2O_4$:Ce^{3+} emits also in the blue–violet region (413 nm) with a duration of more than 10 h, and an invention was provided for generating selected colors by using several acceptor ions for persisting energy transfer [6,7]. Co-doping different rare-earth ions increases the intensity and persistence of $CaAl_2O_4$-based phosphors [8]; substitution of Ca/Sr in place of Ba aluminates resulted in enhanced afterglow emission from Ce^{3+} ions without or with changing the spectral profile [9]; while PL results show a blue shift in the luminescence of Sr substituted $BaAl_2O_4$:Eu^{2+},Dy^{3+} [10].

Decay properties of strontium aluminates improve with Al/Sr ratios and B_2O_3 addition [11,12]; Ce doped $Sr_4Al_{14}O_{25}$ shows a UV emission at 400 nm [13]; B_2O_3 works as a flux by consuming the intermediate phases in the sintering process and also increases the depth of the traps in the ceramic. Improvements in brightness and persistence were further achieved by doping ions like Mg^{2+}, Zn^{2+}, K^+ and Na^+, because this reduces the charge defects induced by substitution of the trivalent rare-earth ions into Sr^{2+} sites within the aluminates [14].

More complex aluminates like Ce^{3+}-doped melilite-based structures have been studied [15]. Crystalline and optical characterization were reported, where broad emission is observed in UV and visible ranges [16], e.g., $Ca_2Al_2SiO_7$:Ce at 410 nm (1–10^3 s) [17], and mechanisms of storing and releasing optical energy is examined in

* Corresponding author. Tel.: +34 913366887; fax: +34 913366836.
E-mail address: fernando.gutierrez@upm.es (F. Gutiérrez-Martín).

0925-8388/$ – see front matter © 2010 Elsevier B.V. All rights reserved.
doi:10.1016/j.jallcom.2010.04.178

order to obtain phosphors with strong intensities and long persistent times [18]. New strontium alumino-silicates showed that the main emission is at an UV area, e.g., $Sr_2Al_2SiO_7$:Ce (387 nm), and $Ca_{0.5}Sr_{1.5}Al_2SiO_7$:Ce,Tb (386 nm); these are first examples of a white long afterglow from single phosphor matrixes [19,20]. The fluorescence of $(Ca_{0.98-x}Sr_x)Al_2Si_2O_8$:$Eu_{0.01}$,$Dy_{0.01}$ shifts from blue to purple (440–406 nm), and its afterglow intensity can be enhanced with an increase of Sr^{2+} concentration [21].

UV-emitting phosphors have been also reported in the context of their applications (e.g., some borates, silicate, phosphates and sulphate), but their decay times are very short [22]. Borate phosphors with high efficiency, easy processibility, durability and long afterglow have attracted attention [23,24], including blue-emitting Ce-activated calcium aluminoborate [25]. Alkaline-earth silicates doped with rare-earth elements show bright and long-lasting phosphorescence in the blue region, especially for $Sr_2MgSi_2O_7$ [26]. $CaMgSi_{2x}O_{6+2x}$:Eu^{2+} showed intense emissions centered around 453 nm, while appropriate Si excess could improve PL intensity [27]. Cerium silicates, such as $Ce_2Si_2O_7$, were the origin of violet/blue luminescence ranging from 358 to 450 nm [28]. The $CdSiO_3$ white light-emitting phosphors may be a new family of materials that show long-lasting phosphorescence ranging from 300 to 700 nm [29–32]. Ce^{3+}-doped lanthanum phosphites show intensive broad emission bands around 340 nm [33].

Phosphors are made generally by solid-state reactions, where the components—typically oxides—are thoroughly mixed and fired for several hours, at temperatures below melting of the mixtures.

Several works deal with using fast combustion methods for large-scale production of phosphors, instead of the standard ceramic techniques with high firing temperatures [34,35]. Long-lasting phosphors can be also synthesized by the sol–gel method which avoids the high temperatures, mineralizers and reducing gases of ceramic routes [36–39]. Methods of combinatorial chemistry in liquid state for the systematic search of phosphors [40], and synthesis of lanthanide doped inorganic–organic materials have also been considered [41].

In conclusion, it is important to find a matrix in which our desired emissions can be obtained by doping with proper ions; it must be noticed that modifications in the processing parameters such as stoichiometric excess of one or more constituents, ion concentration, nature of fluxes, type of reducing atmospheres or the addition of other components can form different crystalline phases and shift the phosphor properties.

After revision of the field, according with our targeted search of the best candidates as photonic sources for TiO_2-activation, the selection and preparation of materials was the first step of our research agenda; then, characterization deals with the most relevant particle properties: i.e., XRD measurements, emissions spectra and decay kinetics; finally, the application tests and scaling of the processes can be carried out.

As seen above, for the systematic search of long phosphorescence materials in the UV region, we should select trivalent rare-earth elements to be introduced in structures of aluminate and/or silicate hosts, which constitute appropriate trap-holes for high phosphorescence materials (it is known that the trapping process involves switching from tri- to tetravalent states of lanthanides, just above the valence band); so, good candidates seem to be those ions that are easily oxidized, with the configuration $4f^{0-7+(1-3)}$.

It could be found that many phosphors emitting in the blue–violet region (~400 nm), with a long-persistence, are related with structures of alkaline-earth alumino-silicates doped with Ce^{+3} ions. Another advantage of these phosphors is that cerium in the most abundant of all the rare-earths, and acts like a highly efficient sensitizing agent. Also, the introduction of different oxides in the host structures might improve the ion emission by crystal effects or other electronic factors; the simultaneous actions of different hosts and concentration of doping ion, aiming at screening of possible mixtures, can be elucidated by design algorithms. Thus, we dealt with such a promising formulation, while still planning further optimisation with all relevant experimental designs. The system includes initially four cations (Ce, Sr, Al, Si), and boron is used as fluxing agent of the sintering phases. Further experiments deal with the effect of Ca + Mg + Ba, as well as flux and doping agents, on photoluminescence efficiency.

2. Experimental

Phosphors were obtained by sintering mixtures of chemicals according to the formula, at proper high temperatures and reducing atmospheres:

$$(Sr_{1-v}M_v)_{1+y}Al_{2-x}B_xSi_yO_{4+3y}:nCe^{3+} \quad (M : Ca, Mg, Ba)$$

The reagents of high purity were weighted in the exact proportions and mixed in a ball-mill for a minimum of half an hour: Al_2O_3, B_2O_3, S_iO_2, $SrCO_3$, $CaCO_3$, $MgCO_3$, $BaCO_3$, $Ce_2(CO_3)_3$. We started with two base formulations made of strontium ($v = 0$) aluminate ($y = 0$) and silicate ($y = 1$), with boron flux ($x = 0.3$), and doped with Ce ($n = 0.01$); these probes were followed by a factorial experiment of 6 parameters at two levels to elucidate the effect of selected composition variables on the three responses (wavelength, intensity and decay of the emission).

Cerium doped polycrystalline samples were prepared by solid-state reaction using stoichiometric amounts of the components, to be heated in a furnace at 1200 °C with ceramic alumina crucibles. The samples were fired at the highest temperature (2 h), under a reducing stream of N_2/H_2 (5%), by using a tubular alumina kiln (HTL-18-50/14 model), with heating elements of SiC (2.5 kW); the temperature program was 5 °C/min, plus 1 h for decomposition of carbonates at 900 °C and 2 h for the solid reactions fired at 1200 °C; finally, they were left to cool in the tube before ground for analysis.

Crystal structures and purity of the samples were tested by X-ray diffraction (XRD) analysis, where the X-ray diffraction pattern was measured using the Cu-Kα radiation (λ = 1.540598 Å) with a Siemens D500 diffractometer equipped with a graphite monochromator. The data were collected at 300 K over an angular range of $10° \leq 2\theta \leq 110°$, by scanning in steps of 0.05° and counting times of 10 s. The results were analyzed by the Rietveld profile refinement method, using the FullProf Suite Program 1.10 (Version Oct-2009).

The photoluminescent spectra (PL) were recorded on a Zeiss MCS-CCD UV-NIR spectrometer, after irradiating the samples with a flash Xenon lamp at room temperature, with a charge time of 5 and 20 s and measurements every second.

3. Results and discussion

3.1. Structural characterization of aluminate and silicate products

Results reported in this section have the main objective to prove that the desired structure of the host lattice was obtained, though we also include several calculations of positional parameters and occupation factors. The distribution of ions and local symmetry may affect the formation of the phase of interest, while the effect of flux promotes the growth of the matrixes and decreases the synthesis temperatures remarkably.

The X-ray diffraction measurements revealed that the samples were a single phase in all cases. The data were indexed in two different crystalline structures, where non silicon samples present distorted monoclinic $SrAl_2O_4$ crystal structures (space group $P12_11$), while the alumino-silicates show a tetragonal $Sr_2Al_2SiO_7$ melilite-type structure (corresponding to the space group $P42_1m$). And, whereas strontium aluminate is a fairly well known system, the alkaline-earth silicates have largely attracted our attention as they have been much less studied and because of their better luminescent properties, higher chemical stability and water resistance.

Then, in order to improve aluminates, which do not show the expected phosphorescence in our application, as seen in Section 3.2, we have investigated different changes in the host structures: first, the matrix is modified with silicate (y); then, we have introduced other alkaline-earths in the host lattice ($v \neq 0$), e.g., calcium (Ca/v), magnesium or barium oxides (Mg/[v – Ca]); on the other hand, the

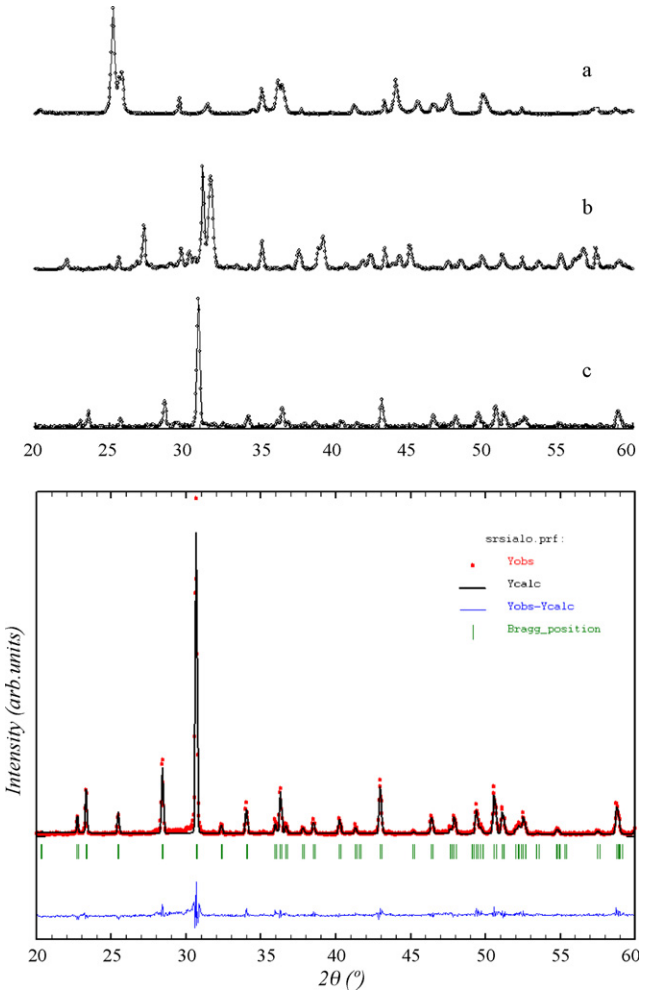

Fig. 1. X-ray powder diffraction pattern for $Sr_2Al_{1.7}B_{0.3}SiO_7$:0.01Ce; (a) initial mixture, (b) after calcined at 900 °C, and (c) sintered at 1200 °C; together with Rietveld analysis (below).

concentration of the doping ion was also varied (n); and finally, the role of the fluxing agent was considered.

In this case, as reported earlier, the Ce doped alkaline-earth alumino-silicates are relatively novel products, which show an intense blue–violet afterglow resulting from single phosphor matrixes. We have analyzed the different XRD patterns, in order to check more carefully the evolution of the samples after the initial calcination and the final solid-state reactions.

Fig. 1 shows the corresponding diffraction data of initial, calcinated and reduced mixtures, made of $SrCO_3 + Al_2O_3 + SiO_2$, with B_2O_3 ($x = 0.3$), and Ce doping ($n = 0.01$), at different temperatures. Typical $Sr_2Al_2SiO_7$ crystal structures appeared at a firing temperature of 1200 °C, and nearly all peaks could be indexed to these phases according to the JCPDS standard card 75-1234. Observed and calculated patterns are shown respectively as dotted and solid lines in the last graphic, where the vertical marks indicate the position of calculated Bragg reflections and traces at the bottom show a plot of the differences between calculated and observed intensities.

In addition, Table 1 lists the atom and crystallographic data as refined by the Rietveld method; in this case, the refinement was performed in the tetragonal space group $P42_1m$, while starting values of the unit cell and positional parameters were those reported for Sr-gehlenite; final cell parameters are: $a = b = 7.8243(2)$ Å, $c = 5.2688(2)$ Å, where the substitution of boron has preference for the Al_3 atomic positions and increases the grid dimensions in the tetrahedral structure made of AlO_4 and SiO_4. These results also indicated that the doping ions, which are far away of their quenching concentrations, had little influence on the grid parameters of the phosphor material, and did not result in the formation of a new phase during the synthesis process.

Table 1
Rietveld refinement results of $Sr_2Al_{1.7}B_{0.3}SiO_7$:0.01Ce.

Atom	x	y	z	Occ.
Sr_1	0.3376(4)	0.1623(4)	0.511(1)	0.499
Al_1	0.00000	0.00000	0.00000	0.232
Al_2	0.143(1)	0.357(1)	0.967(3)	0.232
B_1	0.00000	0.00000)	0.00000	0.018
B_2	0.143(1)	0.357(1)	0.967(3)	0.018
Si_1	0.143(1)	0.3576(1)	0.967(3))	0.250
O_1	0.50000	0.00000	0.143(7)	0.250
O_2	0.142(3)	0.358(3)	0.268(4)	0.500
O_3	0.078(2)	0.159(2)	0.8268(3)	1.000

Cell parameters: $a = b = 7.8243(2)$, $c = 5.2688(2)$, alfa = beta = gamma = 90.00000.
Bragg R-factor: 12.3, Rf-factor = 8.09, Chi2: 3.89.

Finally, a perspective view of the tetragonal phase is given in Fig. 2, which shows the crystal structure of $Sr_2Al_{1.7}B_{0.3}SiO_7$. This compound is crystallized in a melilite-type structure, forming regular networks of AlO_4 and SiO_4 tetrahedra, where the emitting ions of Ce^{3+} may be distributed on the sites of strontium which are located in a two-dimensional arrangement; when Ce^{3+} was doped into the host, it was likely to substitute for the Sr^{2+} ions which have similar radii instead of substituting for the Al^{3+} which has a much smaller ionic radius.

The long-persistence of cerium emissions could be thus originated from charge compensation of doping Ce^{3+} into divalent cation sites, which often causes the generation of defect related traps; and since the 5d energy level is usually close to the host conduction bands, interactions between electrons and the host are very strong and can generate luminescence from red to UV due to the strong crystal field dependence of 5d–4f transition energies.

3.2. Optical measurements

The PL emission spectra of doped strontium aluminosilicate ($Sr_2Al_{1.7}B_{0.3}SiO_7$:0.01Ce^{3+}) show a broad band centered at 400 nm, with approx. 50% of the emission in the desired UVA region; this peak correspond to the transition $^2D_{3/2}$ ($5d^1$) → ^2F_j ($j = 7/2, 5/2$) of Ce^{3+}, and the intensity of luminescence increases with the irradiation time (though differences are not very significant). The persistence of the emissions last for more than two minutes, with a fast initial decay and first-order kinetic rates of approximately 0.10 s^{-1} (Figs. 3 and 4); these properties are considered enough for application in our case (i.e., converting the excitation energy of an

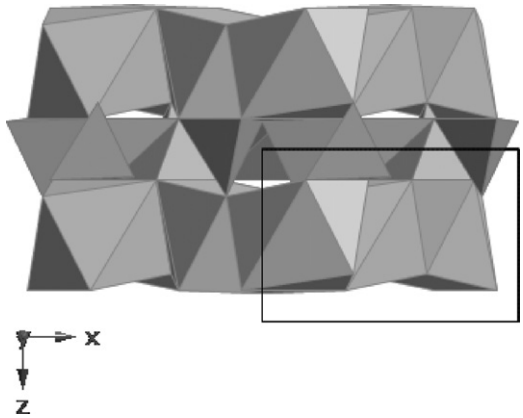

Fig. 2. Crystal structure along [0 1 0] of $SrAl_{1.7}B_{0.3}SiO_7$, distributed in a two-dimensional arrangement (the unit cell is marked).

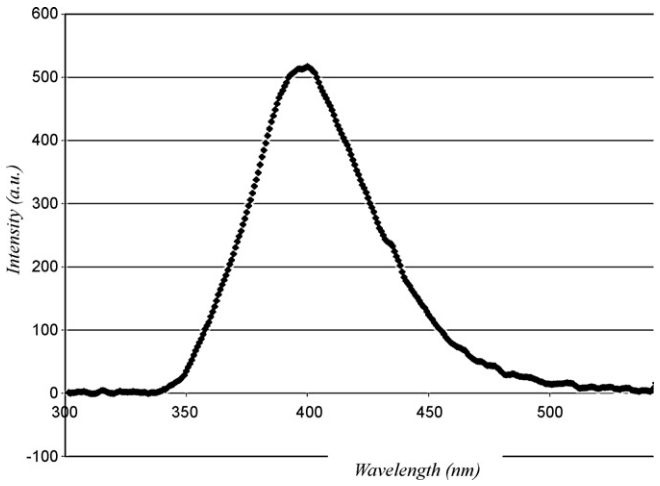

Fig. 3. Emission spectra of $Sr_2Al_{1.7}B_{0.3}SiO_7$:0.01Ce, fired in a reducing atmosphere (5% H_2/N_2).

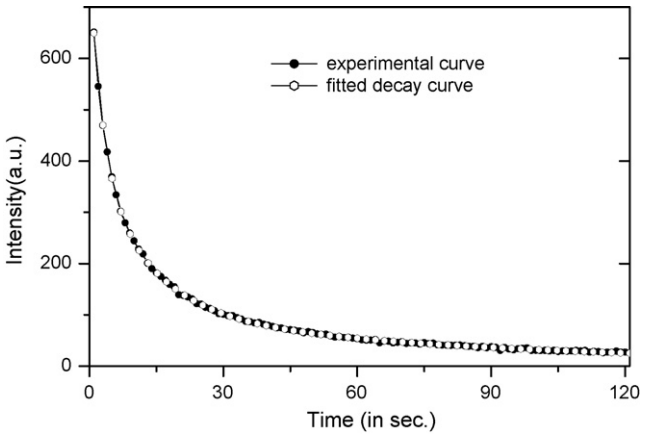

Fig. 4. Decay kinetics of reduced samples $Sr_2Al_{1.7}B_{0.3}SiO_7$:0.01Ce, monitored at λ_{max} = 396 nm.

external source in suitable phosphor emissions which are capable to activate TiO_2 in a cyclic irradiating and photo-catalytic process).

The decay curve of $Sr_2Al_{1.7}B_{0.3}SiO_7$:0.01Ce^{3+} monitored at 396 nm is shown in Fig. 4, and we have fitted the experimental data using the minimum number of first-order exponential terms, which are three straight lines in a logarithmic scale ($I_t = I_0 e^{-t/\tau}$). The intercepts of these lines give the initial intensity values (I_0), while slopes provide the mean lifetimes (τ); the results of the components are tabulated below:

Component	Rate constant (τ)	Initial intensity (I_0)
Fast	2.82 s	375.4
Medium	12.69 s	306.7
Slow	85.51 s	104.0

Looking on possible mechanisms, Ce^{3+} functions as an efficient emission center because 4f–5d transitions of Ce^{3+} allow parity: the emitting Ce^{3+} ions may be distributed on the sites of Sr, located in a two-dimensional arrangement; thus, excitation causes transition of Ce^{3+} from 4f to 5d levels, where electrons reach the conduction band and relax to metastable states; while holes forming Ce^{4+} are trapped in the matrix of AlO_4 and SiO_4 tetrahedra (melilite-type structures), which seem to play an important role in the formation of trap-holes responsible of long-lasting luminescence (see Fig. 5 and related reference).

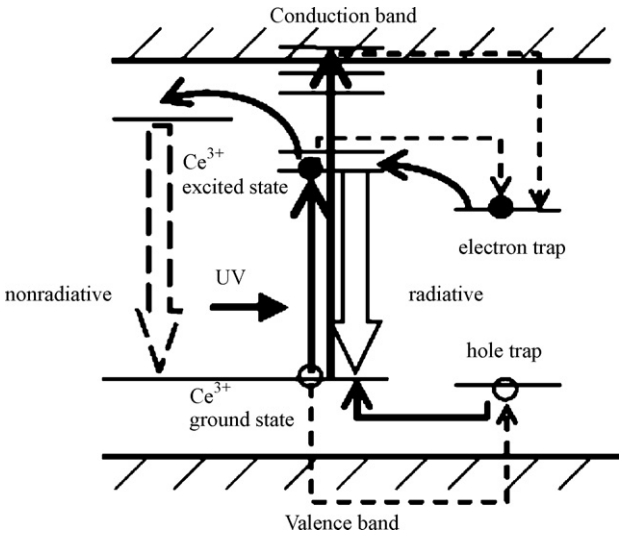

Fig. 5. Phosphorescence process illustration of $M_2Al_2SiO_7:Ce^{3+}$ [18].

The inverse intensity of the phosphorescence seems to increase in proportion to time, and this dependence can be related to a model based on electron–hole recombination at trap centers [16]; the released energy that occurs through a thermally activated process is transferred to Ce^{3+} ions, leading to their characteristic emissions. The 5d states of Ce^{3+} are close to the conduction band, so that it is easy for Ce^{3+} to lose an electron to the conduction band, become Ce^{4+} and exhibit an electron trapping mechanism [42].

A tentative theory of energy differences among rare-earth ions was developed based on survey of literatures related to 4f–5d transitions of ions in various hosts [43], though the nature of their positions in the band gap and the influence on its structure has not been clearly understood yet. Further investigations are necessary to clarify the mechanisms of long-lasting phosphorescence in these materials, though the main objective of this work, as stated in Section 1, was to search the best phosphor formulation by looking at the performance of particles over the compositional space.

Thus we have planned a factorial experiment with six parameters at two levels, which are used as screening tool to elucidate the effect of a number of composition factors on selected responses, with a combinatory statistical approach and minimum experimental trials (as detailed in Table 2). The experiment comprises 12 samples, which were formulated according the composition table of the Plackett–Burman design, and were sintered at 1200 °C under the reducing atmosphere as previously described; the optical measurements confirmed that only the silicated samples ($y = 1$) show the characteristic phosphorescence within the UV region, which is the prime objective of this work as mentioned above (Table 3).

After irradiating the samples with the excitation source, the maximum emission is located in the region between 390 and 405 nm, with only minor differences of the distinct host lattices, which have been modified by the introduction of other alkaline-earth elements in addition to the strontium aluminosilicate; the

Table 2
Experiment of Plackett–Burman with six factors at two levels and three responses.

Factors (X_j)		Unit	Level (−)	Level (+)	Responses (b_{jk})		
1	$y = SiO_2/Al_2O_3$	mol	0	1	b_{11}	b_{12}	b_{13}
2	$v = MO/(1+y)$	mol	1/4	1/2	b_{21}	b_{22}	b_{23}
3	$Ca/v = CaO/MO$	mol	0	1	b_{31}	b_{32}	b_{33}
4	$MgO/[v - CaO]$	mol	0	1	b_{41}	b_{42}	b_{43}
5	$n = 2Ce_2O_3/Al_2O_3$	mol	0.01	0.02	b_{51}	b_{52}	b_{53}
6	$x = B_2O_3$	mol	0.2	0.4	b_{61}	b_{62}	b_{63}

Responses: $k = 1$ (emission: λ, nm) $k = 2$ (luminance: I, a.u.) $k = 3$ (persistence: t, s.).

Table 3
Emission peaks and decay rates of $(Sr_{1-\nu}M_{\nu})_2Al_{2-x}B_xSiO_7:Ce^{3+}$.

Samples		λ_{max} (nm)	$k = \ln 2/t_{1/2}$ (s^{-1})
01	$SrMgAl_{1.6}B_{0.4}SiO_7:0.02Ce^{3+}$	402	0.019
02	$Sr_{1.5}Ca_{0.5}Al_{1.8}B_{0.2}SiO_7:0.02Ce^{3+}$	401	0.046
04	$SrCaAl_{1.8}B_{0.2}SiO_7:0.01Ce^{3+}$	400	0.050
05	$SrBaAl_{1.6}B_{0.4}SiO_7:0.01Ce^{3+}$	393	0.069
06	$Sr_{1.5}Ba_{0.5}Al_{1.8}B_{0.2}SiO_7:0.02Ce^{3+}$	396	0.060
10	$Sr_{1.5}Ca_{0.5}Al_{1.6}B_{0.4}SiO_7:0.01Ce^{3+}$	394	0.077

changes in the intensity (or luminance) of the samples is not significant in this experiment, because the conditions of measurements were not comparable (thus, we have normalized the data in all measurements associated to Table 3). Finally, persistence was shown to improve notably with the addition of magnesium, boron and cerium, as proved by sample 01, with a half-live higher than 30 s and decay rates of about 0.02 s^{-1} (meaning that it is two to four times more persistent than the other samples).

As a final remark, the probes of application of the phosphors in photo-catalytic processes will be the objective of further development in a pilot plant which is now in construction in a laboratory managed by European partners in Frankfurt am Main (Germany); nevertheless, preliminary trials of phosphorescent substances and TiO_2, suspended in aqueous phase with a synthetic organic substrate (rodamine), showed an increase of the degradation after activating the phosphors by an external radiation source (UV lamp).

4. Conclusions

Cerium doped $MO–Al_2O_3–SiO_2$ systems have been investigated, showing interesting luminescent properties for TiO_2-activation in photocatalysis: the UV emission may be obtained from Ce^{3+}, while for long-lasting traps are needed, i.e., hosts like aluminate–silicate doped with suitable sensitizer will lead to the phosphor. Thus, long afterglow pigments have been prepared by solid-state reactions and the samples were characterized for structural and luminescent properties to search the best phosphor formulation according with our particular objective.

Phosphors were synthesized by a simple process of grinding and heating the mixtures at 1200 °C for 2 h in a reducing atmosphere, and long-lasting luminescence near 400 nm was observed in $M_2Al_2SiO_7:Ce^{3+}$ (M:Sr,Ca,Mg,Ba) without any impurity ion other than emission centers of Ce^{3+}. All XRD patterns revealed the expected structure from the solid-state reactions, though only the silicate compounds show the desired phosphorescence when they were sintered in a reducing atmosphere. The emissions of these samples in the near UV region are attributed to $4f \rightarrow 5d$ transitions from Ce^{3+}, with a decay rate which shows the phosphorescence effect; as indicated earlier, this is one of the first examples of short wavelength emitting phosphors obtained from a simple matrix.

Two points were crucial: the reduction of Ce^{4+} to Ce^{3+} achieved by thermal treatment in a reducing atmosphere and the necessity to incorporate boron to increase the fraction of the desired phases. The performance of particles and trends in the responses, studied over the compositional space, show only minor variations of the relevant properties (specially the position of emission bands); though the persistence can be improved by proper selection of the host components and doping concentrations (which could guide the search of phosphors for specific applications).

References

[1] F. Clabau, X. Rocquefelte, T. Le Mercier, P. Deniard, S. Jobic, M.H. Whangbo, Chem. Mater. 18 (2006) 3212–3220.
[2] V. Singh, T.K.G. Rao, J.J. Zhu, J. Lumin. 128 (2008) 583–588.
[3] D. Haranat, V. Shanker, H. Chander, P. Sharma, J. Phys. D: Appl. Phys. 36 (2003) 2244–2248.
[4] F. Clabau, X. Rocquefelte, S. Jobic, P. Deniard, M.H. Whangbo, A. Garcia, T. Le Mercier, Chem. Mater. 17 (2005) 3904–3912.
[5] D. Jia, W.M. Yen, J. Lumin. 101 (2003) 115–121.
[6] D. Jia, X.J. Wang, W. Jia, W.M. Yen, J. Appl. Phys. 93 (2003) 148–152.
[7] W.M. Yen, D. Jia, W. Jia, X.J. Wang, Long persistent phosphors and persistent energy transfer technique, US Patent Appl. 20040164277 A1.
[8] Y. Lin, Z. Tang, Z. Zhang, C. Nan, J. Eur. Ceram. Soc. 23 (2003) 175–178.
[9] N. Suriyamurthy, B.S. Panigrahi, J. Lumin. 127 (2007) 483–488.
[10] H. Ryu, B.K. Singh, K.S. Bartwal, Physica B 403 (2008) 126–130.
[11] A. Nag, T.R.N. Kutty, J. Alloys Compd. 354 (2003) 221–231.
[12] Y.L. Chang, H.I. Hsiang, M.T. Liang, J. Alloys Compd. 461 (2008) 598–603.
[13] S.H. Han, Y.J. Kim, Opt. Mater. 28 (2006) 626–630.
[14] S.D. Han, K.C. Singh, T.Y. Cho, H. Lee, D. Jakhar, J.P. Hulme, C.H. Han, J.D. Kim, I.S. Chun, J. Gwak, J. Lumin. 128 (2008) 301–305.
[15] T. Aitasalo, P. Deren, J. Hölsä, H. Jungner, J. Krupa, M. Lastusaari, J. Legendziewicz, J. Niittykoski, W. Strek, J. Solid State Chem. 171 (2003) 114–122.
[16] N. Kodama, T. Takahashi, M. Yamaga, Y. Tanii, J. Qiu, K. Hirao, Appl. Phys. Lett. 75 (1999) 1715–1717.
[17] M. Yamaga, Y. Tanii, N. Kodama, T. Takahashi, M. Honda, Phys. Rev. B: Condens. Matter Mater. Phys. 65 (2002), 235108.1–11.
[18] M. Yamaga, N. Kodama, Mechanisms of storing and releasing optical energy in long-persistent phosphors of Eu^{2+}- or Ce^{3+}-doped oxides, unpublished.
[19] M. Hosoume, K. Toda, K. Uematsu, M. Sato, 11th Asian Symposium on Ecotech., Dec., 4–5, 2004.
[20] Y. Ito, A. Komeno, K. Uematsu, K. Toda, M. Sato, J. Alloys Compd. 408–412 (2006) 907–912.
[21] Z. Wang, Y. Wang, P. Zhang, X. Fan, G. Qian, J. Lumin. 124 (2007) 140–142.
[22] D.S. Thakare, S.K. Omanwar, P.L. Muthal, S.M. Dhopte, V.K. Kondawar, S.V. Moharil, Phys. Status Solidi A 201 (2004) 574–581.
[23] V.Z. Mordkovich, A.G. Umnov, T. Inoshita, in: J. McKittrick, B. Di Bartolo K. Mishra (Eds.), Luminescent Materials, Mater. Res. Soc. Symp. Proc., vol. 560, Warrendale, PA, 1999, pp. 209–214.
[24] A. Ivankov, J. Seekamp, W. Bauhofer, J. Lumin. 121 (2006) 123–131.
[25] H. Yang, C. Li, H. He, G. Zhang, Z. Qi, Q. Su, J. Lumin. 124 (2007) 235–240.
[26] K. Toda, Y. Imanari, T. Nonogawa, J. Miyoshi, K. Uematsu, M. Sato, J. Ceram. Soc. Japan 110 (2002) 283–288.
[27] Z. Zhang, Y. Wang, J. Lumin. 128 (2008) 383–386.
[28] W.C. Choi, H.N. Lee, Y. Kim, E.K. Kim, in: J. McKittrick, B. Di Bartolo, K. Mishra (Eds.), Luminescent Materials, Mater. Res. Soc. Symp. Proc., vol. 560, Warrendale, PA, 1999, pp. 227–232.
[29] Y. Liu, B. Lei, C. Shi, Chem. Mater. 17 (2005) 2108–2113.
[30] B. Lei, Y. Liu, Z. Ye, C. Shi, Chin. Sci. Bull. 48 (2003) 2434–2437.
[31] B. Lei, Y. Liu, J. Liu, Z. Ye, C. Shi, J. Solid State Chem. 177 (2004) 1333–1337.
[32] B. Lei, Y. Liu, Z. Ye, C. Shi, J. Lumin. 109 (2004) 215–219.
[33] D. Xiong, M. Li, W. Liu, H. Chen, X. Yang, J. Zhao, J. Solid State Chem. 179 (2006) 2571–2577.
[34] V. Singh, T.K. Gundu Rao, J.J. Zhu, J. Solid State Chem. 179 (2006) 2589–2594.
[35] H. Chander, D. Haranath, V. Shanker, P. Sharma, J. Cryst. Growth 271 (2004) 307–312.
[36] M. Marchal, P. Escribano, J.B. Carda, E. Cordoncillo, M. Vallet, F. Conde, J. Sánchez, J. Sol-Gel Sci. Technol. 26 (2003) 989–992.
[37] J. Sánchez-Benítez, A. de Andrés, M. Marchal, E. Cordoncillo, M. Vallet Regi, P. Escribano, J. Solid State Chem. 171 (2003) 273–277.
[38] P. Escribano, M. Marchal, M.L. Sanjuán, P. Alonso-Gutiérrez, B. Julián, E. Cordoncillo, J. Solid State Chem. 178 (2005) 1978–1987.
[39] W. Pan, G. Ning, Y. Lin, X. Yang, J. Rare Earths 26 (2008) 207–210.
[40] K.S. Sohn, S.Y. Seo, H.D. Park, Electrochem. Solid-State Lett. 4 (2001) H26–H29.
[41] B. Julián, R. Corberán, E. Cordoncillo, P. Escribano, B. Viana, C. Sánchez, J. Mater. Chem. 14 (2004) 3337–3343.
[42] D. Jia, J. Lumin. 117 (2006) 170–178.
[43] D. Jia, X. Wang, W. Jia, W.M. Yen, J. Lumin. 119–120 (2006) 55–58.